A Computer-Aided Screening Solution for the Identification of Diabetic Neuropathy From Standing Balance by Leveraging Multi-Domain Features

Alessandro Mengarelli, *Member, IEEE*, Andrea Tigrini, *Member, IEEE*, Federica Verdini, *Member, IEEE*, Mara Scattolini, *Graduate Student Member, IEEE*, Rami Mobarak, *Graduate Student Member, IEEE*, Laura Burattini, *Member, IEEE*, Rosa Anna Rabini, and Sandro Fioretti, *Member, IEEE*

***Abstract*— The early diagnosis of diabetic neuropathy (DN) is fundamental in order to enact timely therapeutic strategies for limiting disease progression. In this work, we explored the suitability of standing balance task for identifying the presence of DN. Further, we proposed two diagnosis pathways in order to succeed in distinguishing between different stages of the disease. We considered a cohort of non-neuropathic (NN), asymptomatic neuropathic (AN), and symptomatic neuropathic (SN) diabetic patients. From the center of pressure (COP), a series of features belonging to different description domains were extracted. In order to exploit the whole information retrievable from COP, a majority voting ensemble was applied to the output of classifiers trained separately on different COP components. The ensemble of kNN classifiers provided over 86% accuracy for the first diagnosis pathway, made by a 3-class classification task for distinguishing between NN, AN, and SN patients. The second pathway offered higher performances, with over 97% accuracy in identifying patients with symptomatic and asymptomatic neuropathy. Notably, in the last case, no asymptomatic patient went undetected. This work showed that properly leveraging all the information that can be mined from COP trajectory recorded during standing balance is effective for achieving reliable DN identification. This work is a step toward a clinical tool for neuropathy diagnosis, also in the early stages of the disease.**

***Index Terms*— Diabetes, peripheral neuropathy, static posture, computer aided diagnosis, machine learning.**

Manuscript received 16 January 2024; revised 29 May 2024; accepted 21 June 2024. Date of publication 26 June 2024; date of current version 3 July 2024. *(Corresponding author: Alessandro Mengarelli.)*

This work involved human subjects or animals in its research. Approval of all ethical and experimental procedures and protocols was granted by the Ethics Committee of the INRCA Hospital, Ancona, Italy, under Application No. 124/2006, and performed in line with the Declaration of Helsinki.

Alessandro Mengarelli, Andrea Tigrini, Federica Verdini, Mara Scattolini, Rami Mobarak, Laura Burattini, and Sandro Fioretti are with the Department of Information Engineering, Università Politecnica delle Marche, 60131 Ancona, Italy (e-mail: a.mengarelli@staff.univpm.it).

Rosa Anna Rabini is with the Department of Diabetology, Mazzoni Hospital, 63100 Ascoli Piceno, Italy.

Digital Object Identifier 10.1109/TNSRE.2024.3419235

I. Introduction

DIABETES is a long-term pathological condition, affecting more than 400 million people worldwide [1], [2], [3], and with a substantial impact on healthcare systems [1], having a rising prevalence on a global level that is estimated to reach about 11% by 2045 [2]. Among possible chronic complications, neuropathy is the most prevalent one, affecting almost 50% of diabetic patients [1], [4]. Diabetic neuropathy (DN) is a degenerative disease that refers to the impairment of autonomic and peripheral nervous systems, targeting sensory, autonomic, and motor axons [1].

The most common type of DN is the symmetric peripheral polyneuropathy (PPN), that affects mainly the distal parts of upper and lower limbs [1], [5]. The involvement of small myelinated fibers can lead to pain in the form of burning or stabbing sensations [6], whereas deterioration of large nerve fibers gives raise to numbness, tingling, and sensory loss [1], [6]. Such kind of symptoms has also a negative impact on the patient quality of life, with detrimental effects on daily activities, and physical and mental issues [1], [6]. Furthermore, PPN is a leading cause of foot ulceration, due to loss of protective sensation that critically weakens the capacity to perceive traumas and high pressure [7]. These late complications can lead to even more serious consequences, as limb amputation, and to an enhanced mortality rate [2], [6].

Considering its degenerative nature, and the absence of specific treatments for nerve fibers impairment [1], [8], an early diagnosis of PPN is paramount in order to enact available options aimed at limiting disease progression [6]. The importance of such aspect is also strengthened by observing that about 50% of PPN occur in an asymptomatic state [6], [7], and thus timely diagnosis would make the patient aware of its condition, easing the planning of anticipatory disease management, as enhanced glycemic control and lifestyle modifications, that require active participation of the patients themselves [1], [6].

Currently, nerve conduction examination is still the most reliable way for diagnosing PPN, also for an early stage of the disease [9]. However, such methods require invasive or uncomfortable interventions, e.g. skin biopsy, laser Doppler scanning of evoked flare, and corneal microscopy [1], that hamper their deployment in clinical routine [1], [8]. Other examinations may be used for assessing fiber functions, as 128-Hz tuning fork and 10-gauge monofilament for vibratory and light-touch perception [1], [6], [10]. Although valid, these simple tests are suited for detecting severe sensory loss and advanced neuropathy only [1], [6], and their usage for identifying mild or initial stages of PPN is not recommended [6], [11]. These aspects lead to a lack of general agreement about screening and diagnosis procedures for clinical practice [4], [6], likely contributing also to the impressive rate of PPN underdiagnosis, in some cases even above 50% [11]. Hence, effective and non invasive diagnostic tools would be valuable to complement existing tests and improve prevention and treatment [1], [11].

Recently, the dramatic growth of computational resources and healthcare data has driven many efforts towards computer-aided solutions for supporting diabetes diagnosis. Most of the studies investigated predictive models for diabetes manifestation, but the learning schemes require clinical and personal information or specific physiological measurements, whose availability is not always guaranteed [12]. Relatively few studies dealt with diabetes recognition and PPN identification [3]. A 10 minutes-long heart rate recordings were needed in [13] for diabetes diagnosis, whereas in [14] PPN detection was pursued by processing corneal confocal microscopy images. Although promising, this kind of methods appear of limited applicability in routine clinical practice, and in addition learning algorithms has to be fed by a large amount of data, whose collection can be challenging [8], [11].

The decline of sensory perception due to PPN, among other complications, has a marked adverse impact on stance stability, with a degraded balance regulation and unsteadiness [10], [15], [16], with an increased risk of fall, recurrent injuries, and fractures [6], [16]. Hence, some previous studies proposed to address the problem of PPN identification by investigating postural steadiness and stance control. Since PPN is peripheral by definition, some attempts have been made by applying image processing to plantar pressure distribution maps, recorded during standing balance and gait, to recognize diabetic subjects with and without PPN [17], [18].

Furthermore, in the past few years, the use of miniaturized, wearable devices, such as inertial measurement units (IMUs), became attractive for the assessment of human motion, due to their portability, reduced dimensions, and affordability [19]. Such devices allow the direct measurement of the acceleration and angular velocity of different body segments, with the possibility to quantify also balance sway when placed on body locations that approximate center of mass position [19]. In particular, inertial sensors were leveraged also for movement analysis of diabetic individuals under a variety of conditions [20]. Only to mention a few, in [21] standing balance of patients with and without PPN was assessed by three bi-axial accelerometers placed on the sacrum and ankle joints. In [22] a single IMU was used for extracting meaningful descriptors of postural sway, and their association with the risk of fall and neuropathy. Wearable inertial sensors were also employed for unveiling differences in gait initiation dynamics between diabetic patients with PPN and healthy elderly [23].

In spite of the validity of the previous technologies, the gold-standard for upright stance maintenance analysis still remains the instrumented posturography, mainly based on the evaluation of the center of pressure (COP) [16], [24]. The latter is the trajectory of the application point of the resultant force exchanged with the ground, thus directly reflecting the amount of postural sway. Also, COP is related to the torque exerted at the lower limb joints, hence encompassing significant information regarding neural and mechanical regulation of balance [15], [24]. For these reasons, COP has been extensively investigated for DN [25], [26], [27], but only few works focused on automated screening solutions aimed at neuropathy identification. The latter was faced in [8], where linear discriminant analysis was fed by global and structural COP parameters, with the former accounting for the magnitude of the sway and the latter for motor control processes. More recently, Villegas et al. [4] explored an aggregation method where COP traces recorded from static and dynamic balance tasks were pooled together for extracting temporal profiles able to distinguish healthy, diabetic, and neuropathic individuals.

All the above mentioned studies gave encouraging results, but none of them considered different degrees of neuropathy severity, preventing their usage for the early recognition of PPN, i.e. before symptoms development [6]. However, findings about the association between COP-based measures, diabetes, and PPN in both asymptomatic and symptomatic stages have been yet reported [10], [25]. Further, due to the non-stationary behavior of COP in quiet standing, classical posturography measures, focused on amplitude and frequency content of COP [24], have been sometimes dismissed in favor of parameters related to nonlinear timeseries analysis. Indeed, such techniques offer a wide range of attractive possibilities, including the description of stochastic dynamics of sway [28], the assessment of fractal and correlation properties [29], [30], [31], and the evaluation of regularity and repeatability of patterns within data [32], [33]. This kind of analyses can provide insights about the neuro-mechanical control of balance [28], [29], [33], and has been successfully exploited also on diabetic patients, in order to explore postural regulation dynamics and their modification due to PPN [15], [27], [34]. However, the effectiveness of such measures in recognizing the presence of PPN in diabetic patients and distinguishing between different stages of the disease has not yet been investigated.

In this study we aimed to provide a computer-aided screening solution for the identification of PPN in diabetic subjects from standing balance. The main contributions can be listed as follows: we proposed to detect PPN by relying on a totally non invasive task, such as upright stance, that was yet investigated for exploring how the presence of diabetes and/or neuropathy affects the neural regulation of balance, but not for achieving an automatic identification of the neuropathic condition [10], [25], [27]. We also tackled the problem of correctly recognizing asymptomatic and symptomatic neuropathy, thus allowing the early recognition of the disease, whereas previous works

pursued the identification of diabetic patients with respect to healthy people [13], [14] or with respect to those affected by neuropathy, but without distinguishing between symptomatic and asymptomatic [4], [8], [17], [18]. For achieving these goals, we leveraged all the information that can be mined from COP time course, by an ensemble of different classifiers trained on different COP components, without relying only on a single component [25], [26], [29], since each of them can add meaningful information without being redundant. Finally, we explored different types of measures computed from COP data, in order to assess whether a combination of features belonging to different domains, i.e. accounting for structural and recurrent pattern within the timeseries, enhances classification performances and disease identification.

II. Methodology

A. Balance Data

Data belonging to a total of 104 subjects affected by type 2 diabetes were retrospectively analyzed [8], [34]: 36 without PPN (NN group), 36 affected by asymptomatic PPN (AN), and 32 with symptomatic PPN (SN). Diagnosis of type 2 diabetes was made by expert physicians of a specialized diabetes outpatient department, according to the current criteria of the American Diabetes Association, and reported in the electronic medical records of the outpatient clinic. No statistically significant differences (ANOVA test) were detected for age, weight, height, body mass index (BMI), and glycosylated hemoglobin (HbA1c) among the three groups ($p > 0.05$, Table I). The patients were selected as age-matched in order to control the influence of the physiological degradation of balance regulation due to aging, by limiting biased conclusions due to the presence of significantly younger or older groups.

Neuropathic condition was assessed through motor and sensory nerve conduction velocity analysis by using electromyography, according to the criteria of the American Diabetes Association [8], [35]. The inclusion within the symptomatic or asymptomatic group was done by expert clinicians by the Diabetic Neuropathy Symptoms Score (DNSS), a clinical questionnaire that provides a score from 0 to 4, and it is considered positive with a value equal or greater than one [36]. Thus, DN patients with a score of 0 were included within the AN group, whereas those who received a DNSS$\geq$1 were labeled as symptomatic (SN group). Subjects belonging to the NN group had a DNSS of 0. The average DNSS of the SN group was 2.55$\pm$0.49. Neurological disorders, peripheral arterial disease, neurotoxic medications, vasculitis, B_{12} vitamin deficiency, renal disease, alcohol abuse, and inflammatory demyelinating neuropathy were ground for exclusion. From an initial cohort of 152 patients, 31 were excluded following the latter criteria. Further, each patient was checked for the absence of factors that can affect balance, such as orthopedic surgery, chronic knee pain or pathology, abnormal gait, active foot ulcers, and retinopathy. On these basis, 17 patients were excluded. None of the remaining ones declined to be enrolled.

Each subject performed the balance task by standing barefoot on a single dynamometric force plate (Kistler 9281), representing currently the gold-standard for the measurement of force exchanged with the ground, satisfying all the standards for medical equipment. The employed force plate has a range of $[-10, 10]$ kN for the planar axes and $[-10, 20]$ kN for the vertical one, a natural frequency of 1 kHz for each axis, and a threshold $<$0.05 N. The COP trajectory in anterior-posterior (AP_c) and medial-lateral (ML_c) directions was recorded at 100 Hz. To limit subject's discomfort, the width of the base of support was kept nearly equal to the pelvis width, and feet were positioned in the same fashion in all the trials, with an average feet-opening angle of 7 ± 4 deg. Posture trials with feet closed together were avoided to not narrowing the base of support, thus introducing additional challenges for balance maintenance [8]. Each patient was able to maintain static balance for at least 120 s. For this study, we considered eyes closed data, due to their higher predictive power, as demonstrated in [8].

TABLE I
Average (Standard Deviation) Values for Anthropometric and Clinical Data. No Statistically Significant Differences Were Found Among the Groups for Any of the Parameters ($p > 0.05$)

Parameters	NN	AN	SN
Age (years)	71.5 (5.1)	69.6 (8.4)	67.4 (10.1)
Height (m)	1.64 (0.07)	1.61 (0.12)	1.64 (0.11)
Weight (kg)	79.1 (13.8)	71.7 (12.0)	74.9 (12.6)
BMI (kg/m^2)	29.3 (5.0)	27.5 (2.8)	27.9 (4.4)
HbA1c (%)	7.3 (0.9)	7.5 (0.8)	7.6 (1.0)

B. Data Processing and Feature Extraction

Center of pressure data were low-pass filtered by a 4^{th} order Butterworth digital filter (cut-off frequency 10 Hz). In order to enhance COP information, in addition to AP_c and ML_c we considered also the statokinesigram (STK_c), i.e. the COP planar displacement [33]. Hence, we computed a total of 21 features, separately from AP_c, ML_c, and STK_c.

Feature set included measures specifically proposed for COP time course together with indices able to quantify the repeatability and complexity of timeseries. More specifically, features can be sorted into three main categories: the first one encompasses the universal descriptors proposed in [24], where an extensive analysis was performed to identify, among 73 COP measures, those that are independent from the individual biomechanics. For AP_c and ML_c, two features were selected by Yamamoto et al. [24] as representative of the neural control of balance, i.e. the slope of the power spectrum at low-frequency band (SL), and the frequency below which is found the 50% of the power spectrum (PS50). From STK_c (Fig. 1(a)), we extracted two additional universal balance descriptors [24], both based on the preliminary computation of the ellipse that encloses the 95% of the statokinesigram: the absolute angular deviation (ANG) between the 95% ellipse and the AP_c direction, and the flattening (FLAT) of the ellipse [24].

The second category of features refers to the modeling of COP fluctuations as a stochastic process. In their seminal work [28], Collins and De Luca proposed a statistical mechanical approach for the assessment of non stationarity in human

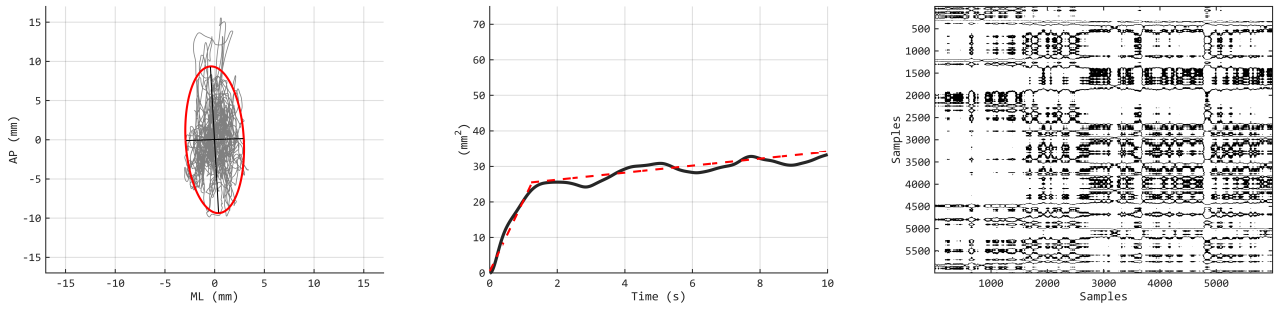

(a) (b) (c)

Fig. 1. Statokinesigram with the 95% ellipse in red (a), stabilogram diffusion function (b), and cross recurrence plot (c) for a representative diabetic patient.

balance sway. This methodology requires the construction of the stabilogram diffusion function (SDF). The typical SDF exhibits two regions (short-term and a long-term) identified by different slopes and separated by a transition point (Fig. 1(b)), where a shift from an open-loop to a closed-loop regulation of balance was advocated [28]. From the transition point, two measures can be extracted: the critical time (CRT), and the mean square displacement (MSD), i.e. the magnitude of the SDF in correspondence of the CRT. Furthermore, in order to have a measure of the stochastic activity over the two SDF regions, the diffusion coefficient can be computed for the short-term (DS) and long-term (DL) regions. Eventually, the persistent or antipersistent behavior of both SDF regions can be quantified by their scaling exponents (HS and HL), which represent the last two features we retrieved from the SDF.

In more recent years, the SDF was further refined in order to account for possible different scaling regimes [37], by parameterizing the log-log SDF curve with a sigmoid-like shape, instead of the originally proposed piecewise approach [28]. In this way, we extracted two additional features: the first one is the variance of the displacement (K) for $\Delta t = 1$ s, that is an estimate of the diffusion coefficient [37]. The other feature is the time-lag (TL) where the nonlinear behavior passes from being persistent to antipersistent, identified as the mid-point of the fitting sigmoid [37]. All the 8 features related to the SDF were extracted from AP_c, ML_c, and STK_c.

The last category of features refers to the repeatability and complexity of the underlining structural patterns of a timeseries. We considered two different tools: the recurrence quantification analysis (RQA) and the sample entropy. The RQA quantifies the deterministic structures and non-stationarity of a timeseries in a reconstructed phase space [38], without making *a priori* assumptions regarding data distribution or stationarity. The RQA is based on the construction of the recurrence plot (RP), which allows to visualize the recurrent dynamics that characterize deterministic, chaotic, and nonlinear systems [30], [38]. Given a N-length timeseries $\mathbf{x}(n)$, its time-delay embedding is performed by building $(N - m + 1)\tau$ vectors, in order to reconstruct the phase space:

$$\mathbf{y}_i^m = \left[x_i, x_{i+\tau}, \ldots, x_{i+(m-1)\tau}\right] \tag{1}$$

where x_i is the i^{th} sample of $\mathbf{x}(n)$, m is the embedding dimension, and τ is a time lag. Then, the RP elements are obtained by computing the geometrical distance $\mathbb{D}_{ij}$ between each pair of embedding vectors $\mathbf{y}_i^m$ and $\mathbf{y}_j^m$:

$$R_{ij} = \Theta(\epsilon - \mathbb{D}_{ij}) \tag{2}$$

where $\Theta(\cdot)$ denotes the Heaviside step function and ϵ is a threshold value for establishing embedding vectors similarity. For computing the distance $\mathbb{D}_{ij}$, we applied the Euclidean norm metric. For the construction of the RP, we selected the embedding dimension $m = 10$, based on the work of Riley et al. [30], where the RQA was applied on COP displacement recorded with the same sampling rate. Following [29], we set the time delay $\tau = 15$, as the lag value for which COP data samples x_i and $x_{i+\tau}$ begin to be not strongly correlated, and the threshold $\epsilon = 30\%$ of the mean distance between data points in the reconstructed space.

The RP can be constructed for a single data sequence, but whether the dependencies between two timeseries has to be assessed, as in the case of the STK_c, a bivariate extension of the RQA is needed. For this purpose, we relied on the cross RQA (CRQA) [38]. This technique was introduced for investigating the simultaneous development of two different trajectories in the phase space, and is particularly suitable when different outputs of a single system are available [38]. The entries of the cross recurrence plot (CRP) are obtained by computing the pairwise distances between each couple of phase vectors ($\mathbf{y}_i^m$ and $\mathbf{z}_j^m$) in the m-dimensional reconstructed phase space:

$$CR_{ij} = \Theta(\epsilon - ||\mathbf{y}_i^m - \mathbf{z}_j^m||) \tag{3}$$

Although visualizing RP and CRP can be useful for retrieving qualitative information (Fig. 1(c)), most often quantitative measures are extracted from their small- and large-scale texture [38]. In this study, we considered ten RQA-based features for AP_c, ML_c, and STK_c. The first one is the recurrence rate (RR), i.e. the number of recurrent points over the total number of RP points, excluding the line of identity. The second one is the determinism (DET), quantified by the number of recurrent points that form a diagonal line, whereas the third one is the ratio (RT) between RR and DET. The average diagonal line length (AVDL) and the maximum diagonal line length (MLL) were also computed. A further feature is the Shannon entropy of the frequency distribution of the diagonal line lengths (ENT), together with the trend (TND), i.e. the

linear regression coefficient over the recurrence points forming diagonals, as a function of the distance from the line of identity. We considered also the laminarity (LAM), whose definition is the same as the DET but considering vertical lines instead of diagonals, the maximum vertical line length (MVL), and the trapping time (TT), i.e. the average length of the vertical lines. We set the minimum length of the diagonal and vertical lines as 4 [29].

Finally, we computed also the sample entropy (SAEN), as a statistics for assessing regularity [39]. The SAEN found an extensive usage for investigating biological signals, including COP time course [32], [34]. In brief, the SAEN is the conditional probability that two m-length embedded vectors, which are similar within a certain tolerance r, remain similar also in a $m+1$ dimensional space. After the embedding procedure, as in (1), the correlation sum is computed:

$$C_i^m(r) = \frac{1}{N-m-1} \sum_{j=1, j\neq i}^{N-m} \Theta(r - \mathbb{D}_{ij}) \tag{4}$$

where $\mathbb{D}_{ij}$ is the Chebyshev distance. Then, the $N-m$ correlation sums defined for each embedding vector are summed up, obtaining $\Gamma_m(r)$. The same procedure is then repeated for $m+1$ and the SAEN is finally computed as the negative logarithm of the ratio between $\Gamma_m(r)$ and $\Gamma_{m+1}(r)$. Regarding the computational parameters of SAEN, for the embedding dimension $m$and time lag τ we selected the same values as for the RQA. The matching tolerance was set as a fraction of the standard deviation of the data, and we selected $r = 0.3$, as in [32]. For the STK_c, we computed the bivariate extension of the SAEN, i.e. the cross sample entropy (CSAEN) [39]. The computation of CSAEN followed the same steps outlined for the SAEN, with the sole difference that the Chebyshev distance is computed between each couple of embedding vectors belonging to the two timeseries [40]. We set the same input parameters used for the SAEN.

In order to avoid dependency from anthropometry, we checked for features having a significant correlation ($\rho > 0.3$ and $p < 0.05$) with at least one anthropometric factor (height or weight), as suggested in [8]. None of the features showed significant correlations.

C. Classification Task

We initially selected five classifiers: k-nearest neighbor (kNN), linear discriminant analysis (LDA), support vector machine (SVM), random forest (RF), and artificial neural network (ANN). These algorithms represent common machine learning models for biological signals classification [8], [37], [41], effective also with low dimensionality datasets. The number of nearest neighbors for kNN was $k = 2$, whereas for SVM we employed a polynomial kernel of order 3. The number of trees in the RF was set as 10 and the growing algorithm was the CART method [42]. The ANN was a feedforward, fully connected neural network, with a single hidden layer. A rectified linear unit and softmax functions were applied to the hidden and output layers respectively.The number of hidden neurons was 5.

For each learning model and classification task, we adopted the leave-one-subject-out (LOSO) validation, where data belonging to one subject are used for testing whereas the remaining data constitute the training set. This process is iterated holding out one subject at a time during the training, until data of each subject have been used once for testing. This kind of cross validation is suited for small datasets and was used in similar studies [8], [41]. Classification was evaluated by using accuracy (AC), precision (PR), sensitivity (SE), and specificity (SP). Feature extraction and classification procedures were performed by using custom-made routines developed with MATLAB R2022b software (Mathworks Inc., Natick, MA, USA). Statistical comparisons were made by using the proprietary functions of the same software.

D. Experimental Setup

1) Experiment-I: In the first experiment we considered NN and SN patients, and the goal was twofold: firstly we aimed at assessing the effectiveness of a feature set that includes metrics specifically designed for describing balance regulation mechanics [24], [28] together with parameters from the timeseries analysis field [38], [39]. The second objective was to investigate which COP component (AP_c, ML_c, and STK_c) provides the best information for classification purposes, and whether one of them should be favored over the others. Our hypothesis was that aggregating the whole information that can be retrieved from the COP time course can be beneficial for PPN identification.

We initially trained the five classifiers separately with the feature set computed on AP_c, ML_c, and STK_c, comparing a total of 15 learning models (5 classifiers $\times$ 3 COP components). Then, we tried to enhance the information retrieved from standing balance in two different ways: in the first one, we augmented the feature space dimensionality, by constructing a set (AUG) made of the single AP_c, ML_c, and STK_c feature sets, initially employed in a separate fashion. In the second way, we combined each learning model by a majority voting ensemble (MVE), where the predictions for each class label are summed up and the final prediction is the class with the highest number of votes [42]. The classifiers used in MVE were those of the same type trained on AP_c, ML_c, and STK_c. Thus, a total of 5 ensemble models were evaluated. The learning model and aggregation scheme which showed the best performances were then retained for the second experiment.

2) Experiment-II: Here, we introduced also the last group, i.e. AN patients, and we firstly considered the latter group together with the SN one, establishing a diabetic neuropathic group (AN+SN). Since AN population shares disease characteristics with both NN (absence of symptoms) and SN (presence of neuropathy), the aim was to investigate the reliability of the solutions gathered during the first experiment for identifying PPN, also when the asymptomatic state of the disease is included. At this stage, four learning models were compared for distinguishing between NN and AN+SN groups. Classifiers were fed with AP_c, ML_c, and STK_c feature sets, in addition to the best aggregation method preserved from the first experiment. In passing, this classification scheme allows comparison with similar works [8].

TABLE II
CLASSIFICATION METRICS FOR THE KNN IN DISTINGUISHING BETWEEN NN AND SN PATIENTS. FEATURE SETS COMPUTED ON AP_c, ML_c, AND STK_c WERE CONSIDERED. IN ADDITION, THE RESULTS FOR THE AUGMENTED FEATURE SET (AUG) AND THE MAJORITY VOTING ENSEMBLE (MVE) ARE ALSO REPORTED

COP component	AC	PR	SE	SP
AP_c	79.4	82.1	71.9	86.1
ML_c	86.8	84.9	87.5	86.1
STK_c	86.8	89.7	81.3	91.7
Aggregation methods				
AUG	91.2	96.4	84.4	97.2
MVE	94.1	96.7	90.6	97.2

Furthermore, we proposed two diagnosis pathways, which have the potential to be used in actual clinical scenarios for supporting PPN screening. The first diagnosis pathway (DP-1) was developed to avoid multiple classification stages and it relies on a single, multi-class, learning model for directly identifying a patient as NN, AN, or SN. The second diagnosis pathway (DP-2) involved two binary learning phases: the first one was devoted to the identification of the symptomatic neuropathy. For this stage, we pooled together NN and AN populations, forming a diabetic asymptomatic group (NN+AN) and the classification involved NN+AN and SN groups. The second step was then finalized to the classification of a subject as non neuropathic or affected by asymptomatic neuropathy.

For each classification mode, we applied a backward feature selection (B-FS) for finding reduced feature sets [41]. The B-FS is a wrapper method that iteratively builds a series of candidate feature sets and the choice is made by a greedy search. From a d-dimensional feature set $\Omega = \{f_1, f_2, \ldots, f_d\}$, a $\Lambda_0 = \Omega$ set is initialized. Then, $d-1$ subsets are constructed, made by all the features in Λ_0 except for one. The feature not present within the subset with the highest accuracy is removed from Λ_0. This process is iterated $d-1$ times, until Λ_0 includes one feature only. The final feature subset is selected as that with the highest accuracy and the lowest dimensionality. In order to limit the possible bias due to this kind of strategy, B-FS was run 50 times by using a random sub-sampling strategy, where the dataset was randomly split in half, and then used for reducing the feature set.

III. RESULTS

In the Experiment-I, the classification accuracy of the five selected classifiers is reported in Fig. 2, where the kNN showed the best outcomes for all the single COP components. The classification metrics for the kNN are listed in Table II. Both aggregation methods (AUG and MVE) boosted the performances of kNN, with accuracy beyond 90%, but MVE outperformed AUG also in terms of sensitivity (84.4% versus 90.6%), resulting overall the best aggregation method. On the other hand, single COP components demonstrated comparable results in identifying NN and SN patients (Table II).

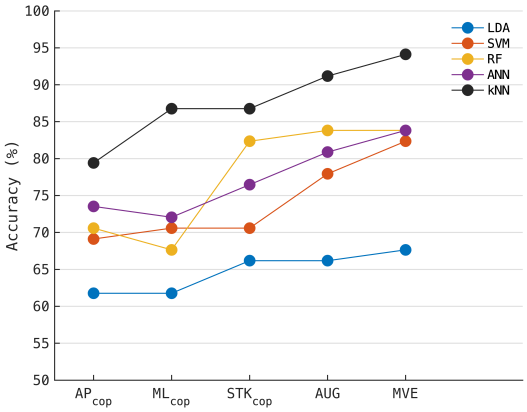

Fig. 2. Classification accuracy for each learning model in distinguishing between NN and SN patients. Feature sets computed on AP_c, ML_c, and STK_c were considered. In addition, the results for the augmented feature set (AUG) and the majority voting ensemble (MVE) are also reported.

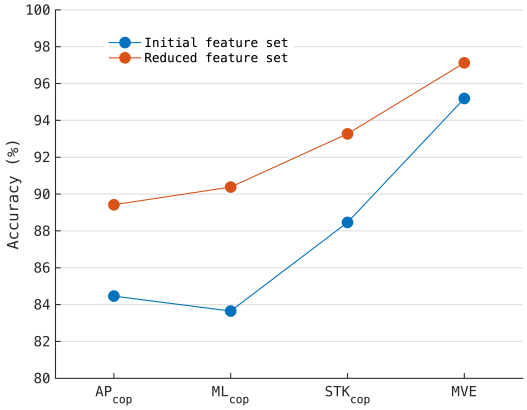

Fig. 3. Classification accuracy of the kNN in distinguishing between NN and AN+SN groups, with the original feature sets and the reduced feature sets, computed on AP_c, ML_c, and STK_c. In addition, the results for the majority voting ensemble (MVE) are also reported.

For what concerns Experiment-II, kNN was retained as classifier and MVE as aggregation method. The feature selection boosted the performances of all the single COP components and of the MVE in distinguishing between patients with and without neuropathy (Fig. 3). Reduced feature sets and detailed classification metrics values are reported in Table III. The DP-1 provided fair results in identifying NN, AN, and SN patients, in particular for the MVE method, but with an accuracy well below 90% (Table IV). Conversely, DP-2 showed high performances for both steps, in terms of all the classification metrics (Table V). The MVE confirmed its value by improving the outcomes given by each single COP component, providing an identification accuracy always above 97% (Table V), misidentifying only 2 out of 32 SN patients in the first step, whereas in the second step none of the AN patients went undetected.

IV. DISCUSSION

A. Experiment-I

The initial feature set, made by a combination of specific descriptors of human balance and metrics related to time-series analysis, proved its suitability for identifying PPN,

and the kNN showed overall the best results in terms of accuracy (Fig. 2), agreeing with other studies focused on the computer-aided identification of pathology from movement data, where kNN outperformed a number of different machine learning models [41]. Further, features computed on STK_c (Fig. 1) resulted the most effective in terms of classification accuracy (Fig. 2), matching with previous works aimed at identifying PPN from balance data, where three out of the five designated features require the STK_c to be computed [8].

However, when dealing with pathological conditions, additional metrics are worth considering for a thorough appraisal of a learning process, beyond classification accuracy. In this view, none of the feature sets computed on AP_c, ML_c, and STK_c gave fully satisfactory results (Table II). The STK_c showed the highest precision and specificity but with a low sensitivity, that represents a fundamental property in clinical contexts, being the goodness of the model in correctly identify a diseased individual. Conversely, ML_c showed a fair specificity, with 5 out of 36 NN patients incorrectly classified as neuropathic but the highest sensitivity (only 4 SN out of 32 went undetected). This matches with previous studies where the transversal COP component was found to be critically affected by PPN [15], [26]. At this stage, none of the three COP components can thus be favored for detecting PPN. This supported our efforts for improving the classification performances, by combining AP_c, ML_c, and STK_c feature sets.

Both the aggregation methods (AUG and MVE) proved to be effective for enhancing the identification of PPN (Table II). On one hand, this supports the hypothesis behind the first experiment, that aggregating the whole information that can be gained from COP time course would improve the neuropathy identification. Indeed, the enhanced performances of AUG or MVE methods likely indicate that even the same type of features, when computed on different COP components, provide complementary rather than redundant information. However, the MVE showed a higher accuracy with respect to AUG and, more importantly, a greater sensitivity, not only with respect to the AUG method but also to each COP component itself (Table II). Hence, for the purpose of this study, a majority voting ensemble of different classifiers resulted a better strategy with respect to a more straightforward increase of the feature set dimensionality.

Although the proposed methodology gave promising results (Table II), two points motivated the additional investigation carried out in the second experiment. Firstly, the MVE of the three kNN fed by different COP components showed a sensitivity not higher with respect to previous studies dealing with the same kind of problem (90.6% versus 92.0%) [8]. Further, within the neuropathy group, only SN patients were considered. However, including also asymptomatic individuals would strengthen the value of the proposed methodology as a possible clinical screening tool, since AN identification based on posturographic data can be a challenging task [8],

B. Experiment-II

The inclusion of the asymptomatic patients within the neuropathic group (AN+SN) did not degrade the classification performances with respect to the first experiment (Fig. 3), thus supporting the validity of the proposed features for PPN identification. In addition, the B-FS algorithm dramatically enhanced the classification performances of each COP component (Table III), being beneficial also for the MVE (Fig. 3).

More in detail, MVE confirmed to be a reliable strategy for combining the classification outputs of single COP components, with a significant improvement also in term of sensitivity and specificity (Table III). In particular, the latter showed limited values, not higher than 89%, when AP_c, ML_c, and STK_c were considered individually (Table III). This aligns with [8] where the SP had a lower value with respect to the other classification metrics, with only 75% of the NN subjects correctly identified. In this view, it is notable that the ensemble of the three single COP components classifiers boosted the SP beyond 94%, with only 2 out of 36 NN subjects mislabeled as neuropathic (Table III), outperforming previous works [8] also in terms of sensitivity (98.5% versus 92.0%). This suggests that the pipeline proposed in experiment 2, where the feature selection step was added before the MVE, was particularly suitable for recognizing the presence of diabetic neuropathy, irrespective of the symptomatic state of the disease.

For what concerns the feature selection phase, two main points are worth noting. Firstly, each reduced set has very few features shared with the other two (Table III), likely indicating that each COP component has its own temporal and spatial characteristics that can be properly mined by means of different descriptors. Further, after the application of the B-FS algorithm, two features resulted present in every reduced set, i.e. HL, SAEN, and CSAEN. This matches with existing literature, where the SDF parameters and entropy measures proved to be effective for analyzing the COP time course [32], [33], also in the case of DN patients [15], [27], [34]. This also confirms the key role played by the long-term dynamics of postural fluctuations for stance regulation, observed using both SDF and entropy based methodologies [15], [27].

Besides, it deserves to be mentioned that RQA metrics represent overall about half of the selected features for the three COP component classifiers (Table III), agreeing well with the value of this timeseries analysis tool for balance investigation [29], [30], [43]. Further, we explored also the bivariate extension of the RQA (Section II-B) for dealing with COP planar path. This represents a novel aspect in the application of RQA to posture data, given that in previous works the most common procedure was to examine AP_c and ML_c separately, without investigating their joint recurrent temporal patterns [31], [43]. Present outcomes support the CRQA for static posture analysis, fostering its application when, and it's almost always the case, simultaneous readings of both COP components are available. Although AP_c is sometimes favored for balance modelling and assessment [44], temporal and dynamical patterns of balance regulation manifest themselves along both directions [15], [26], [27] and thus quantifying their simultaneous evolution and couplings can add meaningful information with respect to treat AP_c and ML_c alone.

The ensemble solution we proposed in Experiment-II enhanced the identification of PPN from posture data also when different type of raw information was examined. The map of the pressure distribution under the feet, treated by image processing techniques, was considered in [18], with performances dependent on the foot sole areas and an average

TABLE III
CLASSIFICATION METRICS FOR THE KNN IN DISTINGUISHING BETWEEN NN AND AN+SN PATIENTS. REDUCED FEATURE SETS COMPUTED ON AP_c, ML_c, AND STK_c WERE CONSIDERED. MAJORITY VOTING ENSEMBLE (MVE) RESULTS ARE ALSO REPORTED

COP component	AC	PR	SE	SP	Reduced feature set
AP_c	89.4	91.3	92.7	83.3	SL, PS50, MSD, DL, HL, K, TL, RR, RT, TND, SAEN
ML_c	90.4	90.3	95.6	80.6	HL, K, RT, AVDL, MLL, TND, MVL, TT, SAEN
STK_c	93.3	94.2	95.6	88.9	ANG, CRT, MSD, DS, DL, HL, TL, RR, AVDL, MLL, TND, MVL, CSAEN
MVE	97.1	97.1	98.5	94.4	

TABLE IV
PERFORMANCES OF THE FIRST DIAGNOSIS PATHWAY (DP-1), MADE BY A SINGLE, MULTI-CLASS CLASSIFICATION STEP. THE LEARNING MODEL IS THE KNN. REDUCED FEATURE SETS COMPUTED ON AP_c, ML_c, AND STK_c WERE CONSIDERED. MAJORITY VOTING ENSEMBLE (MVE) RESULTS ARE ALSO REPORTED

COP component	AC	PR	SE	SP	Feature set
AP_c	76.9	77.2	76.7	87.3	SL, DL, HL, K, RT, TND, TT, MVL, SAEN
ML_c	75.0	76.4	75.6	86.0	PS50, CRT, DL, RR, RT, AVDL, SAEN
STK_c	77.9	78.5	77.7	87.4	FLAT, CRT, MSD, DS, DL, HL, K, TL, AVDL, MLL, ENT, TND, TT, MVL, CSAEN
MVE	86.5	87.6	86.6	93.0	

accuracy of about 95%, and in [17] where a 93.7% accuracy was joined to a relatively low specificity (below 85%).

Our binary pipeline remains valid also if compared with existing solutions that leveraged deep learning. Convolutional neural networks (CNN) fed by several health records provided about 86% accuracy in predicting diabetes [45], whereas incorporating knowledge extension to CNN achieved over 95% accuracy [46], still slightly lower with respect to present results (Table III). The same performances were showed also when a CNN was combined with long short-term memory and a SVM classifier, and applied to heart rate variability data [13]. Beyond their performances, it is remarkable that, in general, the above mentioned methods require to collect a large amount of clinical and non-clinical predictors from the patients [45], [46], or they have to undergo to prolonged recording sessions for collecting enough data [13]. Instead, the methodology we proposed is based on a totally unobtrusive motor task that can be easily performed by patients also outside clinical settings. Also, the learning models we adopted are poorly demanding in terms of computational burden, making the proposed solution suitable also for contexts with limited resources.

C. Diagnosis Pathways

In Experiment-II we proposed two diagnosis pathways, with the the final goal of refining further the neuropathy recognition procedure described above, by distinguishing also between two disease conditions, i.e. symptomatic and asymptomatic.

In DP-1 we attempted to achieve the identification of NN, AN, and SN patients by applying a 3-class classification procedure. Also in this case the MVE offered substantial improvements, enhancing all the classification metrics in comparison to the single COP components alone (Table IV). However, alongside a good capability in recognizing symptomatic neuropathy (87.5% of SN patients were correctly identified), DP-1 failed in providing a reliable detection of the asymptomatic neuropathy (almost 20% of AN patients were misclassified), aligning with [8], where the incorrect classification of neuropathic individuals involved AN subjects only. Present results showed also that, out of 7 misclassified AN patients, 4 were labeled as NN and 3 as SN, likely indicating that ANs share postural attributes with both the other groups, and confirming that their identification based on balance data can be challenging [8], [10]. In spite of performances in line with previous works dealing with similar multi-class problems [17], DP-1 resulted not fully satisfactory with respect to the goal of producing a more powerful tool, able to recognize also different stages of PPN.

Hence, we proposed a second diagnosis pathway made by two binary classification steps. The objective of the first step was to identify the presence of symptomatic neuropathy (SN group) with respect to either asymptomatic or non neuropathic patients (NN+AN group). The same architecture presented before (B-FS followed by MVE) confirmed to be reliable (Table V), with only 3 out of 104 patients being misclassified, and only 2 out of 32 SN patients incorrectly recognized. The good performances of this first classification step likely mirror the substantial impact of PPN on balance regulation, that affects sensory and motor nerves, with an impaired somatosensory perception, leading to modified strategies for upright stance maintenance and postural instability [16]. Thus, PPN symptoms denote an advanced stage of the disease, where balance deterioration is worsened not only in comparison to NN subjects but also with respect to the AN ones, making the identification of SN patients from static posture particularly effective. This aligns well with the presence in each reduced feature set of the universal balance descriptors, that account for the active neuro-mechanical control of quiet standing [24].

The second step of DP-2 showed high performances already for AP_c, ML_c, and STK_c (Table V), but also in this case the MVE demonstrated to be an effective strategy: overall, only 2 out of 72 patients were mislabeled, and both of them were NN individuals incorrectly identified as AN. Moreover, none of the asymptomatic neuropathic patients went undetected, leading to a 100% sensitivity that makes the proposed procedure with the potential to be a valid screening tool. Indeed, the correct identification of asymptomatic PPN in a totally non invasive way has a specific clinical value, given that it would allow the early diagnosis of the disease, enabling to enact timely therapeutic strategies aimed at avoiding symptoms insurgence and the worsening of pathology.

In light of these observations, it is remarkable that this outcomes were achieved by comparing AN patients with the

TABLE V
PERFORMANCES OF THE SECOND DIAGNOSIS PATHWAY (DP-2). THE FIRST STEP IS THE CLASSIFICATION BETWEEN ASYMPTOMATIC (NN+AN) AND SYMPTOMATIC (SN) PATIENTS. THE SECOND STEP IS THE IDENTIFICATION OF A PATIENT AS NN OR AN. THE LEARNING MODEL IS THE KNN. REDUCED FEATURE SETS COMPUTED ON AP_c, ML_c, AND STK_c WERE CONSIDERED. MAJORITY VOTING ENSEMBLE (MVE) RESULTS ARE ALSO REPORTED

First step: (NN+AN) − SN

COP component	AC	PR	SE	SP	Reduced feature set
AP_c	93.3	90.3	87.5	95.8	PS50, HL, K, TL, RT, MLL, TT, SAEN
ML_c	92.3	85.3	90.6	93.1	SL, PS50, DL, TL, RR, MVL, TT, SAEN
STK_c	91.4	96.0	75.0	98.6	FLAT, CRT, DS, DL, HL, K, TL, RR, AVDL MLL, MVL, CSAEN
MVE	97.1	96.8	93.8	98.6	

Second step: NN − AN

COP component	AC	PR	SE	SP	Reduced feature set
AP_c	90.3	93.9	86.1	94.4	CRT, DS, HL, K, TL, RT, AVDL, MLL, TND, TT, MVL, SAEN
ML_c	90.3	89.2	91.7	88.9	MSD, HL, RR, RT, MLL, TND, TT, MVL, SAEN
STK_c	93.1	89.7	97.2	88.9	ANG, DS, DL, HL, TL, RT, AVDL, TT, CSAEN
MVE	97.2	94.7	100	94.4	

NN ones. Indeed, these two groups showed similar levels of postural stability when assessed by classical COP descriptors related to its geometrical and spectral content, leading to a lack of meaningful differences between groups [8], [10]. Unlike the previous step of DP-2, here very few structural features were preserved by the B-FS, i.e. only ANG for the STK_c classifier (Table V), supporting their lower effectiveness for recognizing mild PPN. At the same time this could indicate that, for the latter purpose, features accounting for COP nonlinear dynamics should be favored, possibly because they reflect subtle changes in postural regulation due to neuropathy, when no functional signs of impairment are yet present [15], [34].

Finally, from the viewpoint of a practical application of the DP-2, it should be noticed that both its steps can be used independently from each other. In particular, if the absence of symptoms has been proven by standard clinical procedures, physician can exploit directly the second step of DP-2 in order to assess the presence of neuropathy.

D. Limitations and Future Work

This work presents some limitations that merit discussion. The three groups of patients were homogeneous in terms of physical characteristics, age, and absence of comorbidities. This was done for limiting as much as possible the undesired influence of factors, other than DN, that could affect balance capabilities. However, in this way the population cannot be considered fully representative of what can be encountered in a daily clinical examination. It is also worth mentioning that postural tasks were performed in a rather standardized way, avoiding configurations that could have introduced additional challenges for upright stance stability, e.g. reducing the base of support by imposing feet closed together. Thus, future works should address these points by introducing a higher degree of variability within the groups in terms of different clinical conditions and balance maintenance configurations, in order to test the robustness of the framework in a scenario closer to what can be expected in real practice.

In this study we did not consider a description of postural impairment by classical posturographic analysis, but enlarging the population by selecting less homogeneous groups can be beneficial also for assessing possible relations between classical measures used for balance assessment and those used in this work, and for exploring how the performances of DN identification vary when including different degrees of postural impairment. In passing, future work should also test the validity of the proposed framework when applied to eyes open data, since the latter represents a more viable balance condition for elderly and impaired subjects.

Lastly, further studies are needed in order to exclude the presence of overfitting or possible bias on the final results, introduced by the strategies adopted for classifier selection and feature reduction, by testing the robustness of the identification framework on a new and independent dataset. This would allow to strength the general validity of the methodology, fostering its actual usage as an aiding tool for medical screening.

V. CONCLUSION

Outcomes of this work suggest static balance as a valuable source of information for the development of automated screening solutions for DN identification. This favors the practical applicability of the architecture we proposed, since upright stance is a simple motor task, well-accepted by the patients, and performed in clinical practice on daily basis. The good results obtained by an ensemble of different classifiers indicate that COP components provide complementary information that can improve neuropathy recognition. Findings of this study represent a first step toward the development of a supporting diagnostic system, informed by balance data, for recognizing DN at different severity levels.

REFERENCES

[1] E. L. Feldman et al., "Diabetic neuropathy," *Nature Rev. Disease Primers*, vol. 5, no. 1, p. 41, 2019.
[2] P. Saeedi et al., "Global and regional diabetes prevalence estimates for 2019 and projections for 2030 and 2045: Results from the international diabetes federation diabetes atlas, 9th edition," *Diabetes Res. Clin. Pract.*, vol. 157, Nov. 2019, Art. no. 107843.
[3] T. Zhu, K. Li, P. Herrero, and P. Georgiou, "Deep learning for diabetes: A systematic review," *IEEE J. Biomed. Health Informat.*, vol. 25, no. 7, pp. 2744–2757, Jul. 2021.
[4] C. M. Villegas, J. L. Curinao, D. C. Aqueveque, J. Guerrero-Henríquez, and M. V. Matamala, "Identifying neuropathies through time series analysis of postural tests," *Gait Posture*, vol. 99, pp. 24–34, Jan. 2023.
[5] T. Tuomi, N. Santoro, S. Caprio, M. Cai, J. Weng, and L. Groop, "The many faces of diabetes: A disease with increasing heterogeneity," *Lancet*, vol. 383, no. 9922, pp. 1084–1094, Mar. 2014.

[6] R. Pop-Busui et al., "Diabetic neuropathy: A position statement by the American diabetes association," *Diabetes Care*, vol. 40, no. 1, pp. 136–154, Jan. 2017.

[7] A. J. M. Boulton, "The pathway to foot ulceration in diabetes," *Med. Clinics North Amer.*, vol. 97, no. 5, pp. 775–790, Sep. 2013.

[8] S. Fioretti, M. Scocco, L. Ladislao, G. Ghetti, and R. A. Rabini, "Identification of peripheral neuropathy in type-2 diabetic subjects by static posturography and linear discriminant analysis," *Gait Posture*, vol. 32, no. 3, pp. 317–320, Jul. 2010.

[9] C. Andersson, P. Guttorp, and A. Särkkä, "Discovering early diabetic neuropathy from epidermal nerve fiber patterns," *Statist. Med.*, vol. 35, no. 24, pp. 4427–4442, Oct. 2016.

[10] U. Oppenheim, R. Kohen-Raz, D. Alex, A. Kohen-Raz, and M. Azarya, "Postural characteristics of diabetic neuropathy," *Diabetes Care*, vol. 22, no. 2, pp. 328–332, Feb. 1999.

[11] G. J. Bönhof, C. Herder, A. Strom, N. Papanas, M. Roden, and D. Ziegler, "Emerging biomarkers, tools, and treatments for diabetic polyneuropathy," *Endocrine Rev.*, vol. 40, no. 1, pp. 153–192, Feb. 2019.

[12] S. R. Velu, V. Ravi, and K. Tabianan, "Machine learning implementation to predict type-2 diabetes mellitus based on lifestyle behaviour pattern using HBA1C status," *Health Technol.*, vol. 13, no. 3, pp. 437–447, Jun. 2023.

[13] G. Swapna, R. Vinayakumar, and K. Soman, "Diabetes detection using deep learning algorithms," *ICT Exp.*, vol. 4, no. 4, pp. 243–246, Dec. 2018.

[14] B. M. Williams et al., "An artificial intelligence-based deep learning algorithm for the diagnosis of diabetic neuropathy using corneal confocal microscopy: A development and validation study," *Diabetologia*, vol. 63, no. 2, pp. 419–430, Feb. 2020.

[15] A. Mengarelli, A. Tigrini, F. Verdini, R. A. Rabini, and S. Fioretti, "Multiscale fuzzy entropy analysis of balance: Evidences of scale-dependent dynamics on diabetic patients with and without neuropathy," *IEEE Trans. Neural Syst. Rehabil. Eng.*, vol. 31, pp. 1462–1471, 2023.

[16] C. T. Bonnet and C. Ray, "Peripheral neuropathy may not be the only fundamental reason explaining increased sway in diabetic individuals," *Clin. Biomechanics*, vol. 26, no. 7, pp. 699–706, Aug. 2011.

[17] U. R. Acharya et al., "Computer-based identification of type 2 diabetic subjects with and without neuropathy using dynamic planter pressure and principal component analysis," *J. Med. Syst.*, vol. 36, no. 4, pp. 2483–2491, Aug. 2012.

[18] R. Periyasamy, T. K. Gandhi, S. R. Das, A. C. Ammini, and S. Anand, "A screening computational tool for detection of diabetic neuropathy and non-neuropathy in type-2 diabetes subjects," *J. Med. Imag. Health Informat.*, vol. 2, no. 3, pp. 222–229, Sep. 2012.

[19] M. Patel, A. Pavic, and V. A. Goodwin, "Wearable inertial sensors to measure gait and posture characteristic differences in older adult fallers and non-fallers: A scoping review," *Gait Posture*, vol. 76, pp. 110–121, Feb. 2020.

[20] L. Brognara, A. Mazzotti, A. Di Martino, C. Faldini, and O. Cauli, "Wearable sensor for assessing gait and postural alterations in patients with diabetes: A scoping review," *Medicina*, vol. 57, no. 11, p. 1145, Oct. 2021.

[21] K. Turcot, L. Allet, A. Golay, P. Hoffmeyer, and S. Armand, "Investigation of standing balance in diabetic patients with and without peripheral neuropathy using accelerometers," *Clin. Biomechanics*, vol. 24, no. 9, pp. 716–721, Nov. 2009.

[22] L. Brognara, M. Sempere-Bigorra, A. Mazzotti, E. Artioli, I. Julián-Rochina, and O. Cauli, "Wearable sensors-based postural analysis and fall risk assessment among patients with diabetic foot neuropathy," *J. Tissue Viability*, vol. 32, no. 4, pp. 516–526, Nov. 2023.

[23] G. E. Kang, H. Zhou, V. Varghese, and B. Najafi, "Characteristics of the gait initiation phase in older adults with diabetic peripheral neuropathy compared to control older adults," *Clin. Biomechanics*, vol. 72, pp. 155–160, Feb. 2020.

[24] T. Yamamoto et al., "Universal and individual characteristics of postural sway during quiet standing in healthy young adults," *Physiolog. Rep.*, vol. 3, no. 3, Mar. 2015, Art. no. e12329.

[25] S. Dixit, A. Maiya, B. A. Shastry, and V. Guddattu, "Analysis of postural control during quiet standing in a population with diabetic peripheral neuropathy undergoing moderate intensity aerobic exercise training: A single blind, randomized controlled trial," *Amer. J. Phys. Med. Rehabil.*, vol. 95, no. 7, pp. 516–524, 2016.

[26] H. Salsabili, F. Bahrpeyma, A. Esteki, M. Karimzadeh, and H. Ghomashchi, "Spectral characteristics of postural sway in diabetic neuropathy patients participating in balance training," *J. Diabetes Metabolic Disorders*, vol. 12, no. 1, pp. 1–8, Jun. 2013.

[27] N. Toosizadeh, J. Mohler, D. G. Armstrong, T. K. Talal, and B. Najafi, "The influence of diabetic peripheral neuropathy on local postural muscle and central sensory feedback balance control," *PLoS ONE*, vol. 10, no. 8, Aug. 2015, Art. no. e0135255.

[28] J. J. Collins and C. J. De Luca, "Open-loop and closed-loop control of posture: A random-walk analysis of center-of-pressure trajectories," *Exp. Brain Res.*, vol. 95, no. 2, pp. 308–318, Aug. 1993.

[29] S. Ramdani, G. Tallon, P. L. Bernard, and H. Blain, "Recurrence quantification analysis of human postural fluctuations in older fallers and non-fallers," *Ann. Biomed. Eng.*, vol. 41, no. 8, pp. 1713–1725, Aug. 2013.

[30] M. A. Riley, R. Balasubramaniam, and M. T. Turvey, "Recurrence quantification analysis of postural fluctuations," *Gait Posture*, vol. 9, no. 1, pp. 65–78, Mar. 1999.

[31] E. Fernandez-Cervantes, L. Montesinos, A. Gonzalez-Nucamendi, and L. Pecchia, "Recurrence quantification analysis of center of pressure trajectories for balance and fall-risk assessment in young and older adults," *IEEE Trans. Neural Syst. Rehabil. Eng.*, vol. 31, pp. 926–935, 2023.

[32] S. Ramdani, B. Seigle, J. Lagarde, F. Bouchara, and P. L. Bernard, "On the use of sample entropy to analyze human postural sway data," *Med. Eng. Phys.*, vol. 31, no. 8, pp. 1023–1031, Oct. 2009.

[33] M. Duarte and D. Sternad, "Complexity of human postural control in young and older adults during prolonged standing," *Exp. Brain Res.*, vol. 191, no. 3, pp. 265–276, Nov. 2008.

[34] A. Mengarelli et al., "Complexity measures of postural control in type-2 diabetic subjects," in *Proc. 41st Annu. Int. Conf. IEEE Eng. Med. Biol. Soc. (EMBC)*, Jul. 2019, pp. 3527–3530.

[35] R. Kahn, "Proceedings of a consensus development conference on standardized measures in diabetic neuropathy. autonomic nervous system testing," *Diabetes Care*, vol. 15, no. 8, pp. 1095–1103, 1992.

[36] J. W. G. Meijer, A. J. Smit, E. V. Sonderen, J. W. Groothoff, W. H. Eisma, and T. P. Links, "Symptom scoring systems to diagnose distal polyneuropathy in diabetes: The diabetic neuropathy symptom score," *Diabetic Med.*, vol. 19, no. 11, pp. 962–965, Nov. 2002.

[37] L. Chiari, A. Bertani, and A. Cappello, "Classification of visual strategies in human postural control by stochastic parameters," *Hum. Movement Sci.*, vol. 19, no. 6, pp. 817–842, Dec. 2000.

[38] C. L. Webber Jr and N. Marwan, *Recurrence Quantification Analysis: Theory Best Practices*. Cham, Switzerland: Springer, 2014.

[39] J. S. Richman and J. R. Moorman, "Physiological time-series analysis using approximate entropy and sample entropy," *Amer. J. Physiol.-Heart Circulatory Physiol.*, vol. 278, no. 6, pp. H2039–H2049, Jun. 2000.

[40] I. Ramírez-Parietti, J. E. Contreras-Reyes, and B. J. Idrovo-Aguirre, "Cross-sample entropy estimation for time series analysis: A nonparametric approach," *Nonlinear Dyn.*, vol. 105, no. 3, pp. 2485–2508, Aug. 2021.

[41] A. Mengarelli, A. Tigrini, S. Fioretti, and F. Verdini, "Identification of neurodegenerative diseases from gait rhythm through time domain and time-dependent spectral descriptors," *IEEE J. Biomed. Health Informat.*, vol. 26, no. 12, pp. 5974–5982, Dec. 2022.

[42] T. Hastie, R. Tibshirani, and J. H. Friedman, *The Elements of Statistical Learning: Data Mining, Inference, and Prediction*, vol. 2. Cham, Switzerland: Springer, 2009.

[43] W. van den Hoorn, P. W. Hodges, J. H. van Dieën, and G. K. Kerr, "Reliability of recurrence quantification analysis of postural sway data. A comparison of two methods to determine recurrence thresholds," *J. Biomechanics*, vol. 107, Jun. 2020, Art. no. 109793.

[44] A. Tigrini, F. Verdini, S. Fioretti, and A. Mengarelli, "Center of pressure plausibility for the double-link human stance model under the intermittent control paradigm," *J. Biomechanics*, vol. 128, Nov. 2021, Art. no. 110725.

[45] S. A. Alex, J. J. V. Nayahi, H. Shine, and V. Gopirekha, "Deep convolutional neural network for diabetes mellitus prediction," *Neural Comput. Appl.*, vol. 34, no. 2, pp. 1319–1327, Jan. 2022.

[46] H. Cheng, J. Zhu, P. Li, and H. Xu, "Combining knowledge extension with convolution neural network for diabetes prediction," *Eng. Appl. Artif. Intell.*, vol. 125, Oct. 2023, Art. no. 106658.

Open Access funding provided by 'Università Politecnica delle Marche' within the CRUI CARE Agreement